# Sliding Mode Control Approach with Integrated Disturbance Observer for PMSM Speed System

Lei Yuan, Yunhao Jiang, Lu Xiong, and Pan Wang

***Abstract*—The research on high-performance vector control of permanent magnet synchronous motor (PMSM) drive system plays an extremely important role in electrical drive system. To further improve the speed control performance of the system, a fast non-singular end sliding mode (FNTSM) surface function based on traditional NTSM control is developed. The theoretical analysis proves that the FNTSM surface function has a faster dynamic response and more finite-time convergence. In addition, for the self-vibration problem caused by high sliding mode switching gain, an FNTSM control method with anti-disturbance capability was designed based on the linear disturbance observer (DO), i.e. the FNTSMDO method was employed to devise the PMSM speed regulator. The comparative simulation and experiment results with traditional PI control and NTSM control methods indicate that the FNTSMDO method could improve the dynamic performance and anti-interference of the system.**

***Index Terms*—PMSM, Fast nonsingular terminal sliding-mode, Disturbance observer, PI control.**

## I. INTRODUCTION

IN recent years, with the development of power electronics technology and the continuous progress of the computing power of control chips, it is possible to realize the seemingly complex but very effective control algorithm, as well as the continuous progress of permanent magnet material technology and new energy electric vehicles, permanent magnet synchronous motor (PMSM) has received extensive attention again [1]. Because of its high efficiency, simple and reliable structure, small size and low loss, it is widely used in national defense, military industry, daily life and other aspects. The PMSM speed control system generally uses a proportional-integral (PI) controller, because it has many advantages, such as its simple structure, high reliability, and parameters are easy to correct. However, PMSM is a typical and very complex multivariable nonlinear system. The reason is that the windings have strong coupling, and the motor parameters change with the long-term operation of the motor. In the case of frequent changes in motor parameters and external load interference, the PI controller cannot meet high-performance requirements such as high control accuracy, fast dynamic response, and strong robustness [2].

In order to obtain better control performance, with the continuous development of control technology, more and more control algorithms are designed and applied to the motor speed loop to replace the traditional PI control, e.g. robust adaptive contro[3]-[4], adaptive control based on backstepping method [5], model predictive control [6]-[7], fuzzy neural network control and other intelligent control algorithms, and sliding-mode control (SMC), etc. Compared with the other control strategies, SMC is a special nonlinear control that has been extensively applied to motion control systems, due to the SMC is simple, reliable, and highly robustness. Nevertheless, its drawback is to suppress external disturbances and parameter variation by increasing the sliding-mode switching gain of sign function. On the one hand, the increase of gain can improve the robustness of SMC, but it will also bring the problem of system chattering problem. In order to improve the control performance of traditional SMC control and weaken the chattering problem of the system, many improved SMC methods are proposed [8]-[16].

Compared with the linear sliding-mode surface, a nonlinear sliding-mode surface is more and more used to improve the dynamic performance of SMC. Terminal sliding mode control is one of the earliest sliding mode control strategies using nonlinear sliding-mode surface, and has the advantage of converging to steady state in finite time[11]-[16]. However, the disadvantage of singular value limits its application. In order to solve this problem, nonsingular terminal sliding mode (NTSM) control using nonlinear sliding-mode surface is proposed, which retains the advantages of terminal sliding mode control and solves the singular value problem. To further improve the convergence speed and adjustment time of NTSM control, the fast nonsingular terminal sliding mode (FNTSM) control strategy came into being [17]. In [18], a constant rate variable slope time-varying SMC scheme was proposed to achieve a fast convergence rate of state variables in NTSM. In [19], a novel exponential time-varying sliding-mode surface is designed to

Manuscript received April 14, 2022; revised June 20, 2022; accepted August 15, 2022. Date of publication March 25, 2023; Date of current version January 11, 2023.

This work was supported in part by the National Natural Science Foundation of China under Grant 51507188 and Doctoral Research Startup Foundation of Hubei University of Technology under Grant XJ2021000302. *(Corresponding author: Yunhao Jiang.)*

Lei Yuan is with the Hubei Collaborative Innovation Center for High-efficiency Utilization of Solar Energy, Hubei University of Technology, Wuhan, 430068, China (e-mail: lei.yuan.v@ qq.com).

Yunhao Jiang is with the Hubei Collaborative Innovation Center for High-efficiency Utilization of Solar Energy, Hubei University of Technology, Wuhan, 430068, China (e-mail: jyh6858@126.com).

Xiong Lu is with the Department of Radar System, Ordnance NCO Academy of Army Engineering University of PLA, Wuhan, 430075, China (e-mail: litubaier@ 163.com).

Pan Wang is with the Hubei Collaborative Innovation Center for High-efficiency Utilization of Solar Energy, Hubei University of Technology, Wuhan, 430068, China (e-mail: 475823353@qq. com ).

Digital Object Identifier 10.30941/CESTEMS.2023.00009

improve the NTSM control performance. However, these two methods make the sliding-mode surface design much more complicated and bring difficulties to practical application.

In order to further improve the anti-disturbance ability of SMC, disturbance observer (DO) method with considering unknown model and external disturbance of PMSM speed control system was proposed in [20]–[22]. In [23], an adaptive NTSM with a DO was proposed to further improve the control performance. In [24], a new type of SMC including differential operator and DO is designed. However, all of the above DOs have their disadvantages, that is, the estimation results of interference completely depend on the prior knowledge of interference, so these shortcomings bring some difficulties to the practical application. Meanwhile, the influence of observer steady-state error on the whole system is not analyzed in detail.

Therefore, in order to achieve better control performance and and improve the anti-disturbance ability of PMSM speed control system, this paper proposes a new FNTSMDO control technology, which combines FNTSM control strategy with DO method. Under the condition of satisfying the non-singularity property of the NTSM method and fast convergence, a general FNTSM sliding-mode surface was designed to obtain that make the system state variable reach the steady state in a shortter time by through theoretical calculation and analysis, and display better robustness by comparing the simulation results of different SMC methods. Meanwhile, in order to solve the influence of motor parameters and load disturbance on the control performance of the FNTSM controller, a DO is designed, and the global stability of the system is analyzed theoretically. In this method, DO is adopted as feedforward compensation to overcome the influence of system parameters and external interference. To further weaken the influence of system chattering, Sigmoid function is used to remove the sign function of traditional SMC. Finally, it is verified by simulation and experiment results that FNTSMDO control algorithm has better control effect than NTSM and PI control.

This paper is organized as following. Section II takes second-order nonlinear uncertain mismatched system as an example, the design process of the FNTSM control algorithm is given, and Lyapunov's qualitative stability theorem shows that the system is stable. Section III derives the employed FNTSMDO control strategy, a DO was designed as a feedforward compensation term of FNTSM control to avoid the effects of system parameters and external disturbances. Section IV verifies the control performance through simulation and experimental results, and Section V summarizes the conclusions.

## II. FNTSM CONTROL

### A. FNTSM Control Design

In order to illustrate the general problems in controller design, it is usually necessary to consider the following 2nd nonlinear uncertain mismatch system

$$\begin{cases} \dot{x}_1 = x_2 \\ \dot{x}_2 = \varphi(x) + \mu(x)u + g(t) \end{cases} \tag{1}$$

where $x = [x_1, x_2]^T$ is the state variable, $u$ represents the control input, and $\varphi(x) = \varphi_n(x) + \Delta\varphi(x)$, $\mu(x) = \mu_n(x) + \Delta\mu(x)$, where $\varphi_n(x)$ and $\mu_n(x)$ are nominal variables while $\Delta\varphi(x)$ and $\Delta\mu(x)$ are indeterminacy variables. $g(t)$ denotes the unknown perturbation variable.

Therefore, the equivalent uncertain variable $\xi(t)$ of the system could be expressed as

$$\xi(t) = \Delta\varphi(x) + \Delta\mu(x)u + g(t) \tag{2}$$

Assuming that the uncertain term $\xi(t)$ is bounded, we could obtain the inequation $|\xi(t)| \le l_g$ where $l_g$>0. The equation (1) could be expressed as

$$\begin{cases} \dot{x}_1 = x_2 \\ \dot{x}_2 = \varphi_n(x) + \mu_n(x)u + \xi(t) \end{cases} \tag{3}$$

In system (3), the traditional NTSM control method proposed in [15] was adopted and the sliding mode surface function could be defined as

$$s = e_1 + \frac{1}{\beta} e_2^{\,p/q} = 0 \tag{4}$$

where $e_1 = x_1 - x_d$ represents the tracking error, $e_2 = \dot{x}_1 - \dot{x}_d$ where $x_d$ is the desired signal, $\beta > 0$, and $p, q$ denote odd positive numbers with the meeting $1 < p/q < 2$, and the adjust time $t_{r1}$ satisfies $t_{r1} = \dfrac{p}{\beta^{q/p}(p-q)} e_1^{(1-q/p)}(0)$.

It can be known from equation (4) that since the SMC is realized by the nonlinear part $e_2^{\,p/q}$, the tracking error of the sliding-mode surface will tend to zero in a limited time, but its establishment time is limited. To effectively reduce the chattering phenomenon and enhance the finite convergence, this paper designed an FNTSM surface function as follows

$$s = e_1 + \frac{1}{\alpha}|e_1|^{\gamma+1} + \frac{1}{\beta} e_2^{\,q/p} \tag{5}$$

where $\alpha > 0, \gamma > 0$. $s = \dot{s} = 0$, i.e., The state variables of the system reach the sliding-mode surface from the initial state. The derivative of (5) could yield the following equation

$$\begin{aligned} \dot{e}_1 &= -\beta^{q/p}(e_1 + \frac{1}{\alpha}|e_1|^{\gamma+1})^{q/p} \\ &= -\beta^{q/p}(e_1 + \frac{1}{\alpha} e_1^{\gamma+1}\,\mathrm{sgn}(e_1)^{\gamma+1})^{q/p} \\ &= -e_1^{q/p}\{\beta(1 + \frac{1}{\alpha} e_1^{\gamma}\,\mathrm{sgn}(e_1)^{\gamma+1})\}^{q/p} \end{aligned} \tag{6}$$

where $\mathrm{sgn}(s)$ denotes sign function.

Assuming the starting moment of any initial state $e(0) \neq 0$ $e(t) = 0$ is $t_r$, i.e. $e(t_r) = 0$. By integrating the two ends of (6), the following expression can be obtained

$$\begin{aligned}\int_{e_1(0)}^{e_1(t_r)} \frac{de_1}{e_1^{q/p}} &= -\int_0^{t_r} \{\beta(1+\frac{1}{\alpha}e_1{}^{\gamma}\,\mathrm{sgn}(e_1)^{\gamma+1})\}^{q/p} d\tau \\ &\le -\int_0^{t_r} \beta^{q/p} d\tau\end{aligned} \tag{7}$$

Thus, the following relationship expression could be obtained

$$t_r \le \frac{p}{\beta^{q/p}(p-q)} e_1^{(1-q/p)}(0) \tag{8}$$

Therefore, the steady-state time $t_r$ along with the FNTSM surface (5) is shorter than that required by the traditional NTSM control.

*Remark 1*: The time required to reach the equilibrium point along the sliding-mode surface (5) from any initial state is shorter than that required by traditional NTSM.

To obtain the controller $u$ in (3), using the arrival condition of SMC, it must be met, i.e., $s\dot{s} < 0$

$$\dot{s} = -k\,\mathrm{sgn}(s) \tag{9}$$

where $k > 0$. Substituting the derivative of (5) into (9), the following expression can be obtained

$$\begin{aligned}-k\,\mathrm{sgn}(s) &= e_2 + \frac{\gamma+1}{\alpha}|e_1|^{\gamma} e_2 + \frac{1}{\beta}\frac{p}{q} e_2{}^{p/q-1}\dot{e}_2 \\ 0 &= e_2 + \frac{\gamma+1}{\alpha}|e_1|^{\gamma} e_2 + \frac{1}{\beta}\frac{p}{q} e_2{}^{p/q-1}\dot{e}_2 + k\,\mathrm{sgn}(s)\end{aligned} \tag{10}$$

Substituting (3) into (10), the controller $u$ could be obtained as

$$\begin{aligned}u = -\frac{1}{\mu_n(x)}(\varphi_n(x) + \beta\frac{q}{p} e_2^{2-p/q}(1+\frac{\gamma+1}{\alpha}|e_1|^{\gamma}) + \\ (l_g + k)\mathrm{sgn}(s) - \ddot{x}_d)\end{aligned} \tag{11}$$

### B. Proof of System Stability

The Lyapunov stability theorem is used to verify the stability of the FNTSM controller designed in this paper, define the Lyapunov function as

$$V_1 = 0.5s^2 \tag{12}$$

Combining (5) and (3), the derivation of (12) could be obtained as follows

$$\begin{aligned}\dot{V}_1 &= s\cdot\dot{s} = s\cdot(x_2 + \frac{\gamma+1}{\alpha}|e_1|^{\gamma} x_2 + \frac{1}{\beta}\frac{p}{q} x_2{}^{p/q-1}\dot{x}_2) \\ &= s\{x_2 + \frac{\gamma+1}{\alpha}|e_1|^{\gamma} x_2 + \frac{1}{\beta}\frac{p}{q} x_2{}^{p/q-1}(\varphi_n(x) + \mu_n(x)u(t) + \xi(t))\}\end{aligned} \tag{13}$$

Assuming that $W = \frac{1}{\beta}\frac{p}{q} x_2{}^{p/q-1}$, and substituting (11) to (13), the following equations are obtained

$$\begin{aligned}\dot{V}_1 &= s\cdot\{x_2 + W(\xi(t) - \beta\frac{q}{p} x_2{}^{2-p/q} - (l_g + k)\mathrm{sgn}(s))\} \\ &= s\cdot W\cdot\left(\xi(t) - (l_g + k)\mathrm{sgn}(s)\right) \\ &= W\cdot\left(\xi(t)\cdot s - l_g|s| - k|s|\right)\end{aligned} \tag{14}$$

Assume $|\xi(t)| \le l_g$ and then (14) meet the following conditions

$$\dot{V}_1 \le -W\cdot k|s| \tag{15}$$

where $p$, $q$ are the odd positive numbers that satisfy $1 < p/q < 2$ and $\beta > 0$. When $x_2$ meets $x_2 \ne 0$, $x_2{}^{p/q-1} > 0$, i.e. $W > 0$, then $\dot{V}_1 \le 0$ is established. Therefore, under the guidance of Lyapunov stability theory, the designed FNTSM controller gradually tends to be stable.

### C. Simulation analysis of FNTSM controller

In this section, to verify that the employed FNTSM method has superior regulation performance than the traditional NTSM, the following system was established.

$$\begin{cases}\dot{x}_1 = x_2 \\ \dot{x}_2 = 0.1\sin(20t) + u\end{cases} \tag{16}$$

To conduct the comparative simulation between FNTSM and traditional NTSM, Matlab/Simulink simulation software was used for system modeling, the system desired signal $x_d$ was set as $x_d$=0, and the initial value of state variables $x(0)$ was set as [$x_1$, $x_2$] = [0.1, 0].

It can be seen from Fig. 1 that the simulation results of FNTSM and traditional NTSM control algorithms have obvious difference. Notably, under the action of traditional NTSM control, the adjustment time of the state variables $x_1$ and $x_2$ are about 1.3s and the adjustment time of FNTSM is about 0.92s, hence the proposed FNTSM control strategy obtains a shorter dynamic response time.

## III. Sliding Mode Speed Control using FNTSM

### A. Sliding Mode Speed Control

The mechanical motion and torque dynamics model of PMSM could be employed as [25], [26].

$$\begin{cases}J\frac{d\omega_m}{dt} = T_e - B\omega_m - T_L \\ T_e = \frac{3}{2} p_n \psi_f i_q\end{cases} \tag{17}$$

where $T_L$ is load torque, $\omega_m$ is the mechanical angular speed, $B$ is viscosity coefficient, $T_e$ is electromagnetic torque, $J$ is the moment of inertia, $i_q$ is q-axis current, $p_n$ is the number of poles pairs, and $\psi_f$ is a permanent magnet flux linkage.

In the design of the speed controller, the state parameters of the system are defined as

$$\begin{cases}\dot{e}_1 = \omega_{\mathrm{ref}} - \omega_m \\ \dot{e}_2 = \dot{\omega}_{\mathrm{ref}} - \dot{\omega}_m\end{cases} \tag{18}$$

where $\omega_{\mathrm{ref}}$ is the speed reference value. Supposing that there is a second-order derivative, $\omega_m$ is the speed actual value.

Taking the derivative of (18) and combining it with (17), it can be obtained as

$$\begin{aligned}\dot{e}_2 &= \ddot{\omega}_{\mathrm{ref}} - \ddot{\omega}_m \\ &= -\frac{B}{J} e_2 - \frac{3p_n\psi_f}{2J}\dot{i}_q + \frac{\dot{T}_L}{J} + \ddot{\omega}_{\mathrm{ref}} + \frac{B}{J}\dot{\omega}_{\mathrm{ref}}\end{aligned} \tag{19}$$

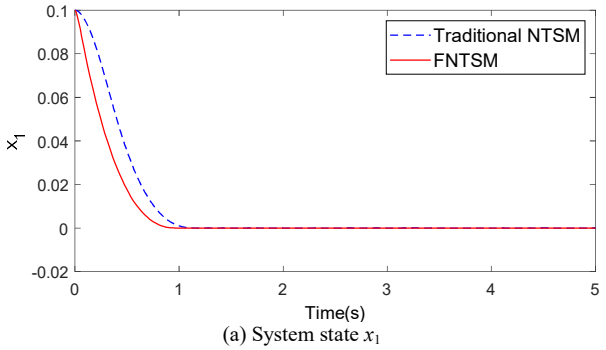

(a) System state $x_1$

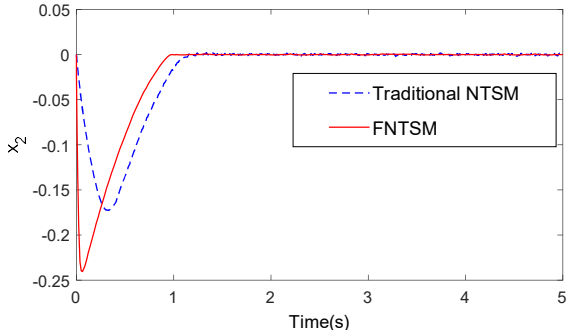

(b) System state $x_2$

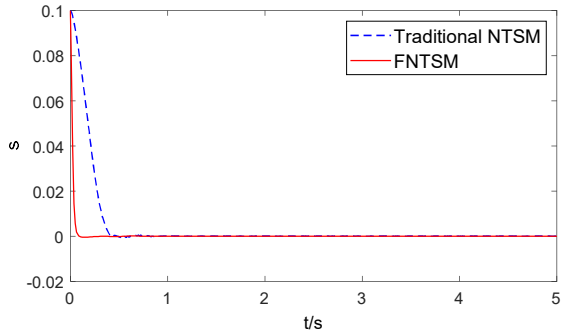

(c) Sliding mode surface $s$

Fig. 1. Performance comparison among FNTSM and traditional NTSM.

Considering the influence of changes in the internal parameters of the motor, formula (18) can be expressed as

$$\dot{e}_2 = (-\frac{B}{J} + \Delta a)e_2 + (-\frac{3p_n\psi_f}{2J} + \Delta b)i_q + (\frac{\dot{T}_L}{J} + \ddot{\omega}_{ref} + \frac{B}{J}\dot{\omega}_{ref} + \Delta c) \quad (20)$$

where $\Delta a$, $\Delta b$, and $\Delta c$ are the uncertain terms.

Assuming that the equivalent uncertain variable is $g(t)$, it could be expressed as

$$g(t) = \Delta a x_2 + \Delta b i_q + (\frac{\dot{T}_L}{J} + \ddot{\omega}_{ref} + \frac{B}{J}\dot{\omega}_{ref} + \Delta c) \quad (21)$$

The motor variables are bounded, hence the disturbance is assumed to be slowly varying load torque disturbance whose differentiation is bounded [27]. The system lumped uncertainty satisfies $|g(t)| \le l_g$, where $l_g > 0$.

Combined with (19), the general mathematical expression of PMSM with uncertain parameters is

$$\begin{cases} \dot{e}_1 = e_2 \\ \dot{e}_2 = -Ax_2 - Bu + g(t) \end{cases} \quad (22)$$

where $A = \frac{B}{J}, B = \frac{3p_n\psi_f}{2J}, u = i_q$. To enhance the dynamic capacity of the speed drive system, the FNTSM control algorithm (11) proposed in Section A was applied to design the FNTSM speed regulation. The controller $u$ was designed as

$$u = \frac{1}{B}\{-Ae_2 + \beta\frac{q}{p}e_2^{2-p/q}(1 + \frac{\gamma+1}{\alpha}|e_1|^{\gamma}) + (l_g + k)\mathrm{sgn}(s)\} \quad (23)$$

To obtain better control performance, the improved function $sig(s) = 2/(1+e^{-a\cdot s}) - 1$ was applied to replace the sign function, where $a$ denotes the positive constant, which has a better performance compared with the sign function applied to sliding mode control [28].

$$u = \frac{1}{B}\{-Ae_2 + \beta\frac{q}{p}e_2^{2-p/q}(1 + \frac{\gamma+1}{\alpha}|e_1|^{\gamma}) + (l_g + k)\mathrm{sig}(s)\} \quad (24)$$

Integrating equation (23), the q-axis current $i_q^*$ is expressed as

$$i_q^* = \frac{1}{B}\int\{-Ae_2 + \beta\frac{q}{p}e_2^{2-p/q}(1 + \frac{\gamma+1}{\alpha}|e_1|^{\gamma}) + (l_g + k)\mathrm{sig}(s)\}dt \quad (25)$$

Therefore, the control block diagram of the FNTSM speed controller is shown in Fig. 2.

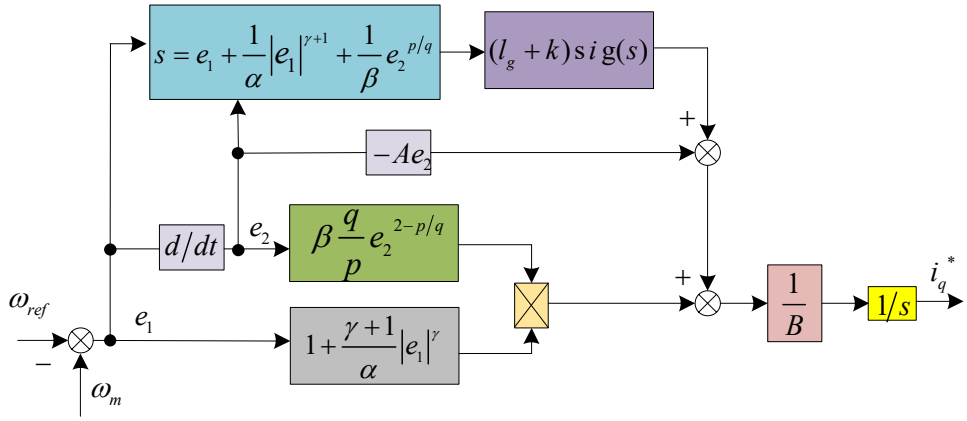


Fig. 2. Block diagram of the FNTSM.

### B. Disturbance Observer Design

It can be seen from (25) that $l_g$ is the gain of the reaching law in SMC, which directly determines the severity of chattering problem and is affected by the $g(t)$. To Improve the anti-disturbance ability of the control system, a DO is employed to estimate $g(t)$ online, and iq* is used to perform feedforward compensation on the estimated $g(t)$.

Assuming that $e_2$ and g(t) are the state variables of (22). The FNTSM speed control with DO could be expressed as

$$i_q^* = \frac{1}{B}\int\{-Ae_2 + \hat{g}(t) + \beta\frac{q}{p}e_2^{2-p/q}(1+\frac{\gamma+1}{\alpha}|e_1|^{\gamma}) + (l_g+k)\mathrm{sig}(s)\}dt \tag{26}$$

The DO could be expressed as

$$\begin{cases}\dot{\hat{e}}_2 = -Ae_2 + \hat{g}(t) - Bu + k_1\tilde{e}_2 \\ \dot{\hat{g}}(t) = k_2\tilde{e}_2\end{cases} \tag{27}$$

where $k_1$, $k_2$ denote the observer gain.

The stability of the designed controller is verified by using Lyapunov function.

$$V = V_1 + \frac{1}{2k_2}\tilde{g}^2 + \frac{1}{2}\tilde{e}_2^2 \tag{28}$$

where $\tilde{g} = g(t) - \hat{g}(t)$, $\tilde{e}_2 = \hat{e}_2 - e_2$ represent the $e_2$ and disturbance errors respectively.

Combining (26), the derivation of (28) could be obtained as

$$\begin{aligned}\dot{V} &= \dot{V}_1 + \frac{1}{k_2}\tilde{g}(\dot{g}-\dot{\hat{g}}) + \tilde{e}_2(\dot{e}_2 - \dot{\hat{e}}_2) \\ &= sW\left(g - \hat{g} - (l_g+k)\mathrm{sig}(s)\right) + \frac{1}{k_2}\tilde{g}(\dot{g}-\dot{\hat{g}}) + \tilde{e}_2(\dot{e}_2 - \dot{\hat{e}}_2) \\ &= sW\left(\tilde{g} - (l_g+k)\mathrm{sig}(s)\right) + \frac{1}{k_2}\tilde{g}(\dot{g}-\dot{\hat{g}}) + \tilde{e}_2(\dot{e}_2 - \dot{\hat{e}}_2)\end{aligned} \tag{29}$$

The switching frequency of the controller is usually high, hence the disturbance is constant within one controller cycle, i.e. $\dot{g} = 0$. Substituting (26) into (28), now the (29) becomes

$$\begin{aligned}\dot{V} &= sW\left(\tilde{g} - (l_g+k)\mathrm{sig}(s)\right) - \frac{1}{k_2}\tilde{g}\dot{\hat{g}} + \tilde{e}_2(\dot{e}_2 - \dot{\hat{e}}_2) \\ &= sW\left(\tilde{g} - (l_g+k)\mathrm{sig}(s)\right) - \tilde{g}\tilde{e}_2 + \tilde{e}_2\left(g - \hat{g} - k_1\tilde{e}_2\right) \\ &= W\left(s\tilde{g} - (l_g+k)|s|\right) - k_1\tilde{e}_2^2 \\ &\le -W\left((l_g+k) - \tilde{g}\right)|s| - k_1\tilde{e}_2^2\end{aligned} \tag{30}$$

$W > 0, k_1 > 0, \tilde{g} \approx 0$, hence the equation (30) is expressed as

$$\dot{V} \le -W(l_g+k)\cdot|s| - k_1\tilde{e}_2^2 \le 0 \tag{31}$$

where the coefficient $k_1$ and $l_g$+$k$ are positive constant gain, which ensure that the designed DO is stable, and the tracking errors converges to zero.

So, the block diagram of the FNTSMDO is presented in Fig. 3.

## IV. Simulation and Experiment Results Analysis

### A. Simulation Analysis

To demonstrate that the applied FNTSMDO speed regulator has better control performance than the traditional PI and NTSM speed control, the vector control strategy with id = 0 in Fig. 4 was employed, and the parameters of the PMSM are shown in Table I.

TABLE I
PARAMETERS OF PMSM

| Parameter and unit | Value |
|---|---|
| Rate power Pn | 0.2kW |
| Rate voltage Vn | 48V |
| Number of poles pairs | 2 |
| Inductance Ld=Lq | 1.378mH |
| Permanent magnet flux linkage $\psi_f$ | 0.0221Wb |
| Stator phase resistance R | 0.3Ω |
| Moment of inertia | $0.175\times10^{-4}$ J/kg.m$^2$ |
| Viscosity coefficient B/ | $0.044\times10^{-5}$ N.m.s/rad |

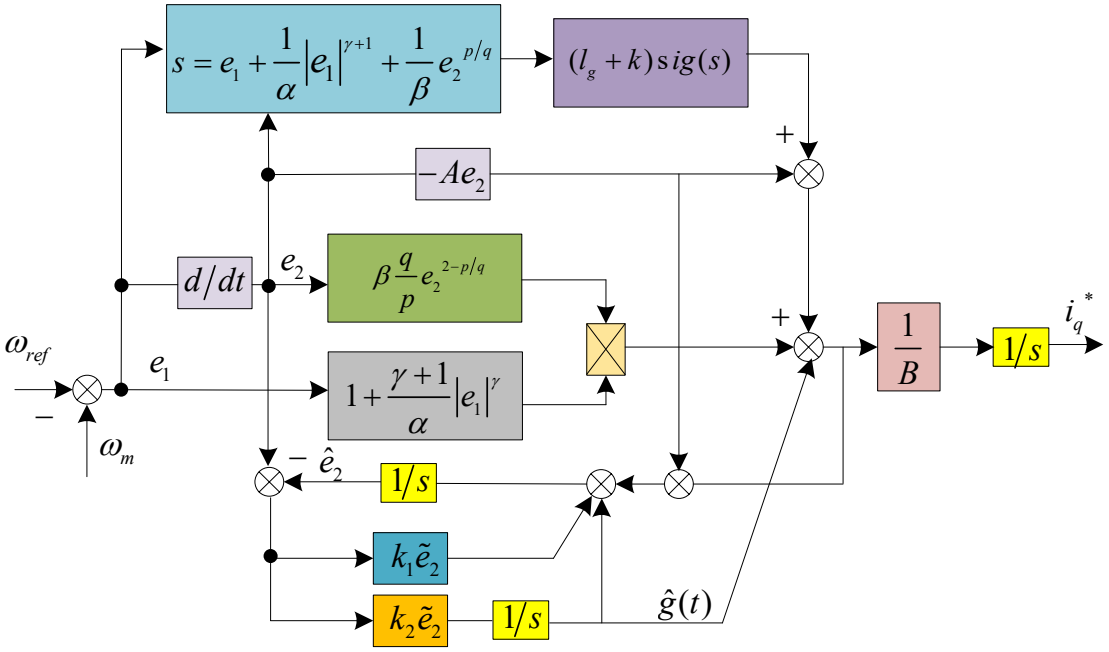


Fig. 3. Block diagram of FNTSMDO.

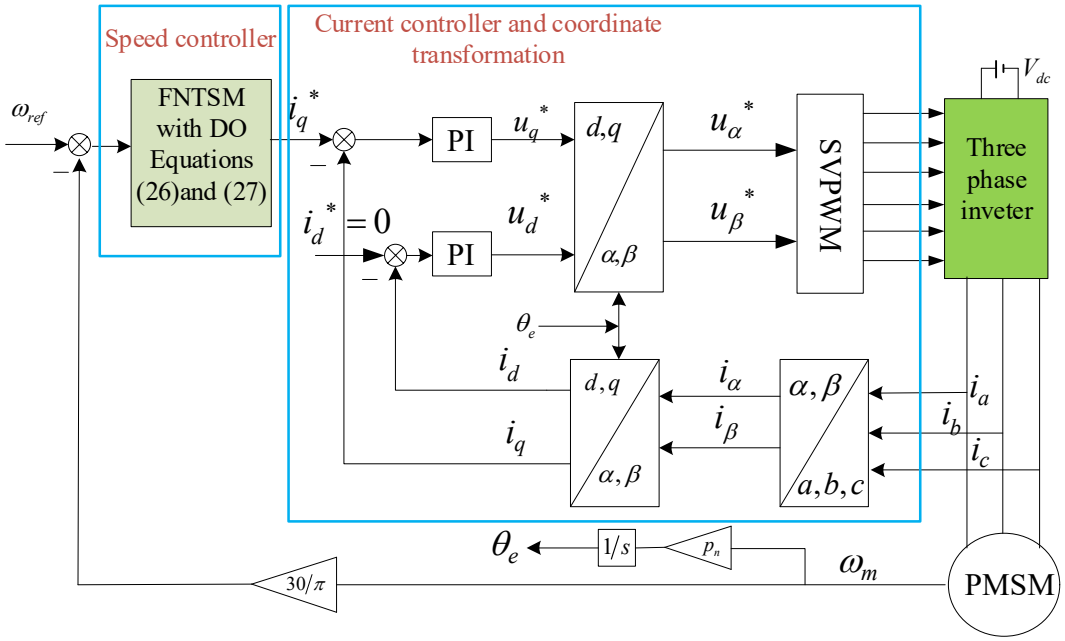


Fig. 4. Block diagram of PMSM speed-regulation system.

To present the comparison and analysis results, the simulation conditions of the three different control algorithms were set as the same. The paramates of speed-loop PI control were set as kpv=0.16,kiv=2, and d- and q-axis currents-loop PI control were set as kpdq=43.5,kidq=3500. The paramates of speed-loop FNTSMDO control were set as $p$=3,$q$=5,$\beta$=0.02, $\alpha$=0.2. Meanwhile, to verify the start-up performance and anti-disturbance capability of the motor, the reference value of the motor speed was set as 1000r/min, the motor is started under no-load state, the load torque was suddenly used at t=0.1 s, and the simulation time was set to 0.2 s. The simulation results under PI control, traditional NTSM control, and the proposed FNTSMDO control are presented in Fig. 5. Fig.5(a), (b), and (c), which show the speed waveform, electromagnetic torque waveform, and three-phase current waveform respectively.

Fig. 5(a) shows the motor speed curve under three different control methods. Notably, when motor start-up under PI control is large, the overshoot of motor speed is about 25.2% and the adjustment time is about 0.04s. When the load torque increases suddenly, the speed of the motor will fluctuate greatly; when the motor returns to the steady-state, the adjustment time is about 0.035s. Moreover, when the traditional NTSM control is adopted, the overshoot of the motor is only about 0.15%, and the adjustment time at start-up and sudden load increase is about 0.025s and 0.02s respectively. Conversely, the motor could run no overshoot under the FNTSMDO's action and the motor speed fluctuation is very small when the load torque suddenly increases. The adjustment time at startup and sudden load increase is about 0.012s and 0.01s respectively. Therefore, FNTSMDO control algorithm has faster adjustment time and better anti-disturbance performance.

Fig. 5(b) ,Fig.5(c) and Fig.5 (d) present the simulation curves of d- and q-axis currents current, electromagnetic torque and three-phase current respectively. In the simulation, the saturator of speed loop regulation was set as ± 5.9A to prevent excessive starting current of the motor, hence the maximum current was 5.9A and the maximum torque was about 1N.m during the motor start-up.

In addition, when the load torque suddenly increases at t = 0.1s, the electromagnetic torque suddenly increases to overcome the change of external load disturbance, as presented in Fig. 5(b). When the electromagnetic torque equals the load torque, i.e. 0.72N.m, the motor regained energy balance and returned its speed to a steady state of 1000r/min. The three-phase current and the three-phase electromagnetic torque are positively correlated, so the three-phase current and electromagnetic torque change are the same. Therefore, it is verified that the FNTSMDO outperforms PI and traditional NTSM in terms of control performance.

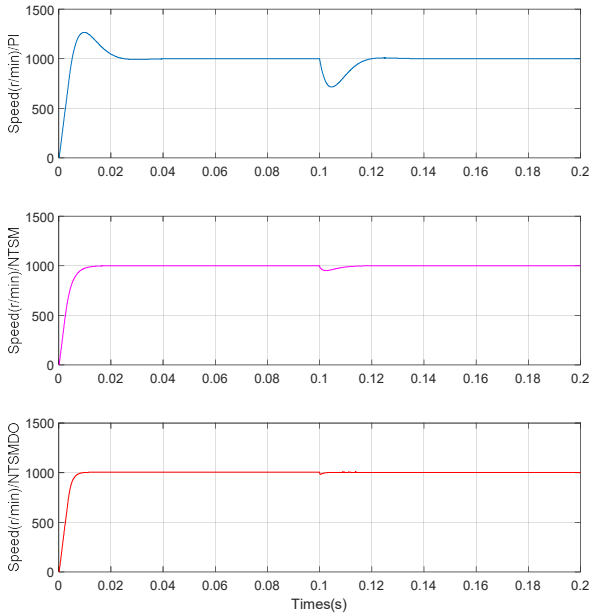


(a) Speed waveform

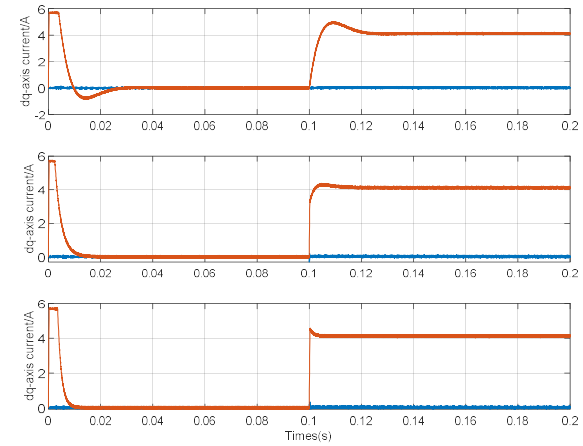


(b) d- and q-axis currents waveform

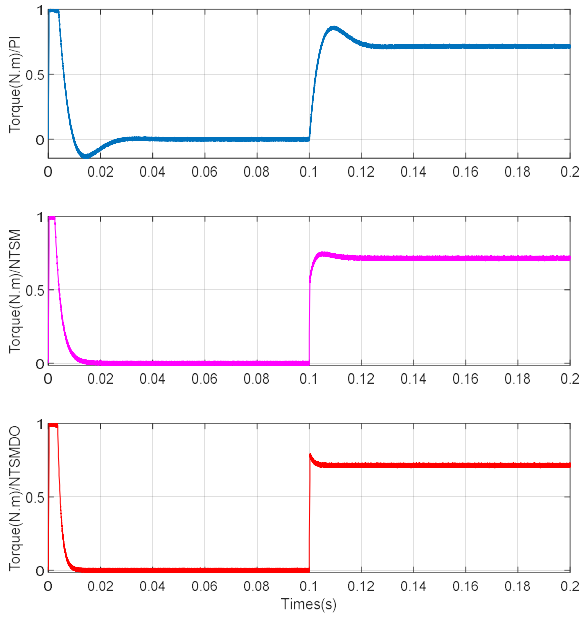


(c) Electromagnetic torque waveform

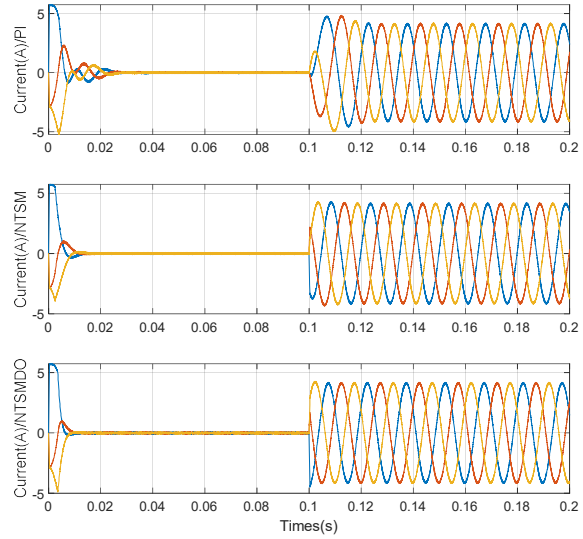


(d) Three-phase current waveform

Fig. 5. Simulation results under three control method

## B. *Experiment Results Analysis*

To further prove the control quality of the FNTSMDO algorithm, an experimental platform as shown in Fig. 6 was built, and an experimental platform of the PMSM system based on DSP (TMS320F28335) was established. The RAM chip was applied to record the experimental data like speed and current. After the platform shut down, the upper computer was applied to collect and process the data and Matlab was employed to draw the experimental waveform.

In this section, the comprehensive experimental results of the motor start-up process and load increase under the action of the three methods (FNTSMDO, NTSM, and PI) are compared and analyzed in detail to prove that the FNTSMDO algorithm has better startup performance and anti-disturbance capability.

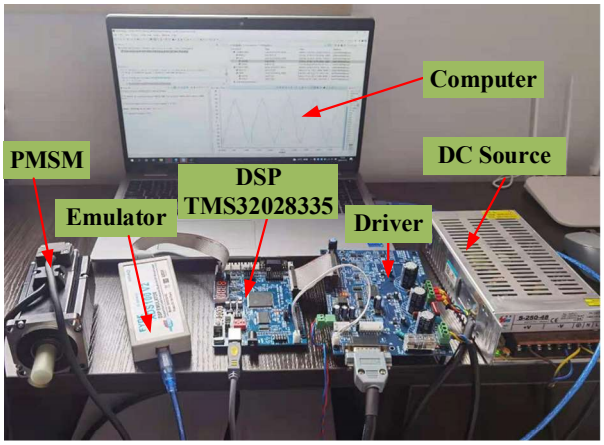


Fig. 6. Experimental platform.

TABLE II
PARAMETERS OF THE START-UP PROCESS

| Control Scheme | OS (%) | Adjustment time (s) |
|---|---|---|
| FNTSMDO | 0 | 0.02 |
| NTSM | 1.3% | 0.04 |
| PI | 17.5% | 0.055 |

TABLE III
PARAMETERS OF LOAD INCREASE PROCESS

| Control Scheme | Speed Fluctuation (r/min) | Adjustment time (s) |
|---|---|---|
| FNTSMDO | 65r/min | 0.015 |
| NTSM | 85r/min | 0.04 |
| PI | 243r/min | 0.05 |

To illustrate the control performance with motor start-up, the experimental PMSM speed reference value was set as 1000r/min, and the startup transient process is shown in Fig.7. As indicated in Fig.7(a), the motor start-up under the PI controller has 17.5% overshoot while the traditional NTSM has 1.3% overshoot. As presented in Fig. 7(b) and (c), the proposed FNTSMDO control strategy shows no overshoot. Moreover, the settling time of the speed under PI, traditional NTSM, and FNTSMDO are about 0.055s, 0.04s, and 0.02s respectively. The detailed experimental results at other speeds are presented in Table II. Compared with PI and traditional NTSM methods, the dynamic characteristics of FNTSMDO control strategy are better.

Given the above, the control characteristics of the motor start-up process has been analyzed. In the following section, the anti-disturbance capability of the three different control

algorithms of the PMSM speed system will be analyzed in detail. Figure 9 shows the test results of PMSM under the stable working condition of 1000r/min, when the load torque is suddenly increased.

As indicated in Fig. 8(a), When the load torque is suddenly increased, the speed of the motor fluctuates significantly; when the motor returns to be stable, the adjustment time operation is about 0.05s.

In contrast, as presented in Fig. 8(b) and (c), under the traditional NTSM and the FNTSMDO control method, when the load torque is suddenly added, The speed fluctuation is

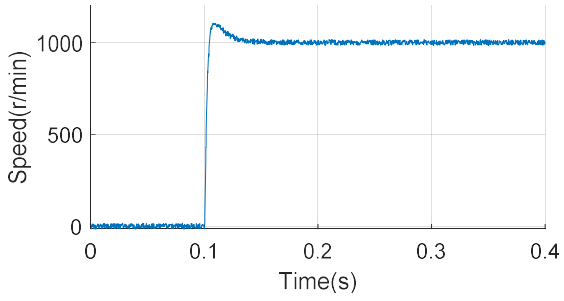


(a) PI control

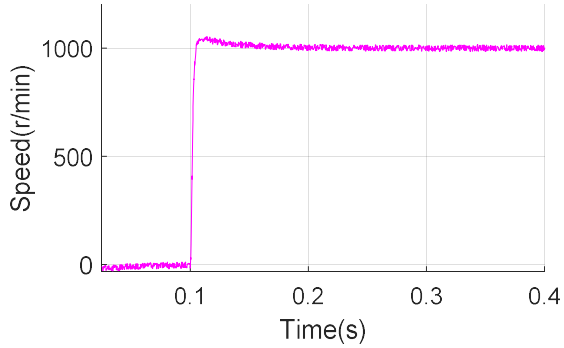


(b) Traditional NTSM control

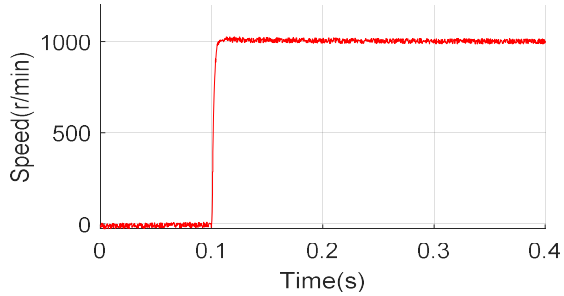


(c) FNTSMDO control

Fig.7. Experimental results during the motor start-up.

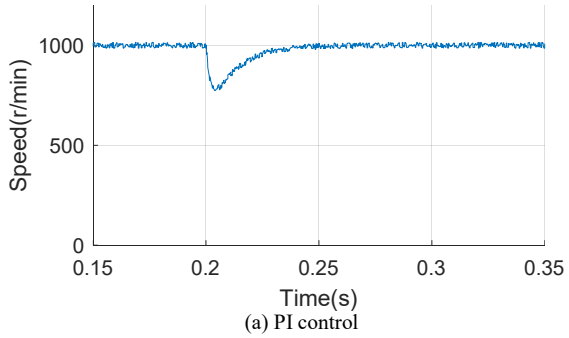


(a) PI control

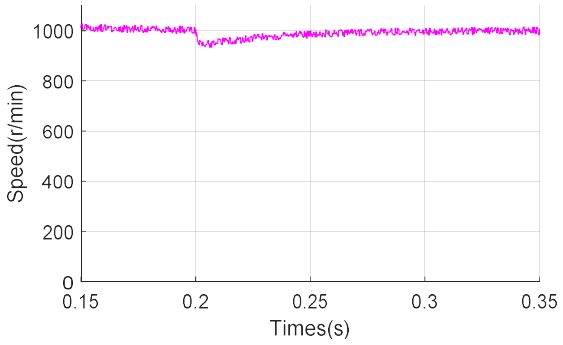


(b) Traditional NTSM control

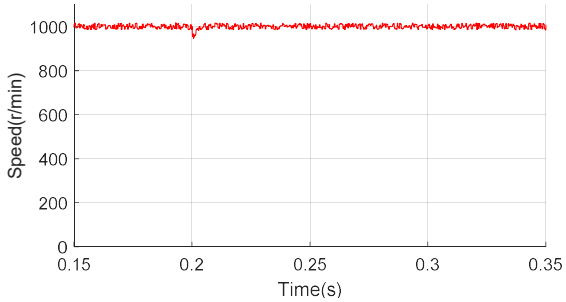


(c) FNTSMDO control

Fig.8. Experimental results when motor load increases.

smaller and the dynamic stabilization time is shorter, about 0.04s and 0.015s, respectively. The detailed experimental comparison results are shown in Table III. Thus, the FNTSMDO has better control quality compared with PI and traditional NTSM.

## V. CONCLUSION

In order to further improve the control performance of PMSM speed control system, a new FNTSM control strategy is proposed based on the traditional NTSM control. This method not only includes the finite time convergence and nonsingular characteristics of NTSM, but also improves the convergence time of the system, it is proved that the FNTSM control algorithm can optimize the convergence characteristics and shorten the convergence time. Meanwhile, the FNTSM algorithm was applied to the PMSM speed system and an FNTSMDO speed control algorithm that combined the FNTSM control with the DO method was employed. The DO was designed as the feedforward compensation item of the q-axis current controller. Finally, the comparison of simulation and experimental results of three control methods shows that the FNTSMDO control algorithm is better in terms of start-up and anti-interference, and significantly improves the control quality of the PMSM drive system.

## REFERENCES

[1] W. Xu, A. K. Junejo, Y. Liu, and M. R. Islam, " Improved continuous fast terminal sliding mode control with extended state observer for speed regulation of PMSM drive system," *IEEE Trans. Indu. Electron.*, vol.68,no.11, pp.10465– 10476, 2019.

[2] L.Yuan, M. L.Chen, and J. Q.Shen, "Current harmonics elimination control method for six-phase PM synchronous motor. *ISA Transactions*,vo.59,pp. 841-849,2015.

[3] X. Zhang, L. Sun, K. Zhao, and L. Sun, "Nonlinear speed control for PMSM system using sliding-mode control and disturbance compensation techniques," *IEEE Trans. Power Electron.*, vol.28, no.3, pp.1358–1365, 2013.

[4] F. Mwasilu and J. Jung, "Enhanced fault-tolerant control of interior PMSMs based on an adaptive EKF for EV traction applications," *IEEE Trans. Power Electron.,* 2016, 31(8): 5746–5758.

[5] P. Tomei, and C. M. Verrelli, "Observer-based speed tracking control for sensorless permanent magnet synchronous motors with unknown load torque," *The XIX International Conference on Electrical Machines*, 6-8 Sept. 2010.

[6] M. Preindl and S. Bolognani, "Model predictive direct torque control with finite control set for PMSM drive systems, Part 1: Maximum torque per ampere operation," *IEEE Trans. Ind. Informat.,* vol.9,no.4,pp.1912–1921, 2013.

[7] Z. Ma, S. Saeidi, and R. Kennel, "FPGA implementation of model predictive control with constant switching frequency for PMSM drives," *IEEE Trans. Ind. Informat.*,vol.10, no.4, pp.2055–2063,2014.

[8] Y. Q. Wang, Y. T Feng, X. G. Zhang and J. Liang, "New reaching law control for permanent magnet synchronous motor with extended disturbance observer," *IEEE Access,* vol.7, pp.186296-186307,2019.

[9] A. K. Junejo, W. Xu, and C. X. Wu, "Adaptive speed control of PMSM drive system based a new sliding-mode reaching law," *IEEE Trans. Power Electron.*, vol. 35,no.11, pp.12110-112121,2020.

[10] Y. Feng, X.Yu, and F. Han, "High-order terminal sliding-mode observer for parameter estimation of a permanent-magnet synchronous motor," *IEEE Trans. Ind. Electron.,* vol.60, no.10, pp.4272–4280,2013.

[11] W. Xu, A. K. Junejo, Y. Liu, and M. R. Islam, "Improved continuous fast terminal sliding mode control with extended state observer for speed regulation of PMSM drive system," *IEEE Trans. Veh. Technol.*, vol.6, no.11, pp.10465-10476,2020.

[12] C. Mu and H. He, "Dynamic behavior of terminal sliding mode control," *IEEE Trans. Ind. Electron.,* vol.65, no.4, pp.3480–3490,2018.

[13] C. Mu, W. Xu, and C. Sun, "On switching manifold design for terminal sliding mode control," *J. Franklin Inst.*, vol.353, no.7, pp.1553–1572, 2016.

[14] S. S. Xu, C. Chen, and Z.Wu, "Study of nonsingular fast terminal sliding mode fault-tolerant control," *IEEE Trans. Ind. Electron.*, 2015, 62(6): 3906–3913.

[15] Feng Y, Man Z, "Non-singular terminal sliding mode control of rigid manipulators," *Automatica*, vol.38, no.12, pp.2159- 2167,2002.

[16] Jin Y Q, Liu X D, and Qiu W, Time varying sliding mode controls in rigid spacecraft attitude tracking," *Chinese Journal of Aeronautics,* vol. no.4, pp.352-360,2008.

[17] Z. Yang, D. Zhang, X. Sun, and X. Ye, ''Adaptive exponential sliding mode control for a bearingless induction motor based on a disturbance observer,''*IEEE Access*, vol. 6, pp. 35425–35434, 2018.

[18] Z. Chen, J. Geng, and X. D. Liu., "An integral and exponential time-varying sliding mode control of permanent magnet synchronous motors," *Trans on China Electro-Technical Society*, vol. 26, no.6, pp. 756-761,2011.

[19] S. S. Xu, C. Chen, and Z.Wu, "Study of nonsingular fast terminal sliding mode fault-tolerant control," *IEEE Trans. Ind. Electron.*, vol.62,no.6, pp.3906–3913, 2015.

[20] D. Nojavanzadeh, M. Badamchizadeh, "Adaptive fractional-order nonsingular fast terminal sliding mode control for robot manipulators," *IET Control Theory Appl.*, vol. 10(13): 1565–1572, 2016.

[21] J. Huang, S. Ri, T. Fukuda, and Y. Wang, ''A disturbance observer based sliding mode control for a class of underactuated robotic system with mismatched uncertainties,'' I*EEE Trans. Autom. Control*, vol. 64, no. 6, pp. 2480–2487, Jun. 2019.

[22] S. Cao, J. Liu, and Y. Yi, ''Non-singular terminal sliding mode adaptive control of permanent magnet synchronous motor based on a disturbance observer,'' *J. Eng.*, vol. 2019, no. 15, pp. 629–634, Mar. 2019.

[23] Z. Zhou, B. Zhang, and D. Mao, ''Robust sliding mode control of PMSM based on rapid nonlinear tracking differentiator and disturbance observer,'' *Sensors*, vol. 18, no. 4, p. 1031, Mar. 2018.

[24] Z. Xiaoguang, Z. Ke, S. Li, and A. Quntao, ''Sliding mode control of permanent magnet synchronous motor based on a novel exponential reaching law,'' *Proc. CSEE*, vol. 31, no. 15, pp. 47–52, May 2011.

[25] S. M.Wasu, U. B. Sarode, and M. P. Bhavalkar, " Speed control of PMSM system using improved reaching law based sliding mode control and disturbance observer technique," *Int. J. Adv. Comput. Res.*, vol.3, no.13, 312–318, 2013.

[26] X. Zhang, L. Sun, K. Zhao, and L. Sun, "Nonlinear speed control for PMSM system using sliding-mode control and disturbance compensation techniques," *IEEE Transactions on Power Electronics*, vol.28,no.3, pp.1358-1365, 2013.

[27] Aishwarya Apte, Vrunda A. Joshi, Hrishikesh Mehta, and Rahee Walambe, "Disturbance-observer-based sensorless control of PMSM using integral state feedback controller," *IEEE Transactions on Power Electronics*, vol.35, no.6, pp.6082-6090, 2020.

[28] L. Yuan, F. Xiao, J. Q. Shen, "Sensorless control of high-power interior permanent magnet synchronous motor drives at very low speed," *IET Electric Power Appl*, vol.7, no.3, pp.199–206, 2013.

**Lei Yuan** received the B.Sc. degree in automation from University of South China, Hengyang, China, in 2008, and the M.Sc. degree in control theory and control engineering and Ph.D. degree in electrical engineering from the PLA Naval University of Engineering, Wuhan, China, in 2010 and 2014, respectively.

He is currently working as a Lecturer with the School of Electrical and Electronic Engineering, Hubei University of Technology, Wuhan, China. He has authored more than 30 technical papers published in journals and conference proceedings. His research interests include power conversion and control technique and its applications in distributed generation, motor drive, and flexible power transmission and distribution.

**Yunhao Jiang** received the M.S. and Ph.D. degrees in electrical engineering from the Huazhong University of Science and Technology, Wuhan, China, in 2006 and 2010, respectively. From 2011 to 2014, he was a lecturer at Nanjing University of Information Science & Technology.

He is currently an Associate Professor in Hubei University of Technology. His research interests include application of power electronics, electromagnetic compatibility of power conversion and interference suppression.

**Lu Xiong** received the B.Sc., M.Sc., and Ph.D. degrees in armament science and technology from the PLA Naval University of Engineering, Wuhan, China, in 2008, 2010 and 2014, respectively.

She is currently working as a Lecturer with the Department of Radar System, Ordnance NCO Academy of Army Engineering University of PLA. Her research interests include armament science and technology, and its applications in distributed motor drive, and flexible power transmission and distribution.

**Pan Wang** received the M.S., and Ph.D. degrees in the School of Electrical Engineering from Wuhan University, Wuhan, China, in 2011, and 2018, respectively.

She is currently a Faculty Member of the School of electrical and electronic engineering, Hubei University of Technology, Wuhan, China. Her current research interests include high-power converters such as medium-voltage motor drives, active power filters, wind power generation and photovoltaic.